

# In-medium meson properties and screening correlators

A. Bazavov<sup>a</sup>, F. Karsch<sup>a,b</sup>, Y. Maezawa<sup>b</sup>, Swagato Mukherjee<sup>a</sup> and P. Petreczky<sup>a</sup>

<sup>a</sup> Physics Department, Brookhaven National Laboratory, Upton, NY 11973, USA,

<sup>b</sup> Fakultät für Physik, Universität Bielefeld, D-33615 Bielefeld, Germany

**Abstract.** We study spatial meson correlation functions consisting of strange quarks, strange and charm quarks and charm quarks in (2+1)-flavor QCD using the highly improved staggered quark action. We find that the in-medium modification of the meson correlators decreases with increasing charm quark content and decreasing size. In particular, we find strong in-medium modification of  $\phi$  and  $D_s$  meson correlators around the chiral transition temperature  $T_c$ , while  $J/\psi$  and  $\eta_c$  correlators show strong in-medium modification only at temperatures of  $1.4T_c$ .

## 1. Introduction

At high temperatures matter controlled by the strong force undergoes a deconfinement transition at which the relevant degrees of freedom change from hadrons to quarks and gluons (see e.g. Refs. [1, 2] for recent reviews). Hadronic correlation functions have been advocated since long as a tool to learn about the properties of this strong interaction matter [3, 4]. They encode the in-medium properties of hadrons and their dissolution. Moreover, through the comparison of lattice results with weak coupling calculations at high temperature [5, 6] they also provide information on the change from strongly to weakly interacting matter. In particular, the modifications of meson correlators in the light and strange quark sector reflect the in-medium change of meson properties and the partial restoration of chiral symmetry. The in-medium modification and dissolution of heavy quarkonium was suggested as the signal for creating a deconfined medium in heavy ion collisions by Matsui and Satz [7]. The existence of heavy light-mesons above the chiral transition temperature has also been proposed to explain the large energy loss and flow of heavy quarks observed in heavy ion collisions [8].

Spectral functions, defined in terms of the Fourier transform of the real time meson correlation functions, provide the most straightforward way to describe in-medium meson properties and their dissolution. Meson states appear as peaks in the corresponding spectral functions with the peak position equal to the meson mass. The width of the peak corresponds to the in-medium width of the meson. However, lattice QCD is formulated in Euclidean space time. Temporal meson correlation functions calculated on the lattice,

$$G(\tau, \vec{p}, T) = \int d^3x e^{i\vec{p}\cdot\vec{x}} \langle J_H(\tau, \vec{x}) J_H(0, \vec{0}) \rangle, \quad (1)$$

have a simple relation to the spectral function,  $\sigma(\omega, \vec{p}, T)$ :

$$G(\tau, \vec{p}, T) = \int_0^\infty d\omega \sigma(\omega, \vec{p}, T) K(\omega, \tau), \quad K(\omega, \tau) = \frac{\cosh(\omega(\tau - 1/2T))}{\sinh(\omega/2T)}. \quad (2)$$

Here  $J_H$  is a meson operator, typically of the form  $J_H = \bar{q}\Gamma_H q$ , with  $\Gamma_H$  being some combination of the Dirac matrices that specifies the quantum numbers of the meson. One way to obtain the spectral function from the above relation is to use the maximum entropy method (MEM) [9, 10, 11, 12, 13, 14, 15, 16]. The analysis of temporal correlation functions is difficult due to the limited extent,  $1/T$ , in Euclidean time direction. In the case of heavy quarkonium correlators, for instance, it turned out that the melting of bound states does not lead to large changes in the correlation functions [17, 16]. In order to become sensitive to the corresponding disappearance of a resonance peak in the spectral function high statistical accuracy and the analysis of the correlation function at a large number of Euclidean time separations is needed. At fixed temperature  $T = 1/N_\tau a$ , this requires large lattices with temporal extent  $N_\tau$  and sufficiently small lattice spacing,  $a$ .

On the lattice one can also study spatial meson correlation functions

$$G(z, T) = \int_0^{1/T} d\tau \int dx dy \langle J_H(\tau, x, y, z) J_H(0, 0, 0, 0) \rangle. \quad (3)$$

These are related to the spectral functions in a more complicated way that also involves integration over the spatial momenta,

$$G(z, T) = \int_0^\infty \frac{2d\omega}{\omega} \int_{-\infty}^\infty dp_z e^{ip_z z} \sigma(\omega, p_z, T). \quad (4)$$

On the other hand the spatial separation is not limited by the inverse temperature and the spatial correlation function can be studied at separations larger than  $1/T$ . Therefore the spatial correlation functions can be more sensitive to in-medium modifications and/or the dissolution of mesons. While the relation between spectral functions and spatial meson correlators is more involved in general, in some limiting cases it becomes simple. At large distances the spatial correlation functions drop exponentially,  $G(z, T) \sim \exp(-Mz/T)$ , where  $M$  is known as the *screening mass*. At small enough temperatures when there exists a well-defined mesonic bound state, the spectral function has the form  $\sigma(\omega, 0, 0, p_z, T) \sim \delta(\omega^2 - p_z^2 - m_0^2)$ , and  $M$  becomes equal to the (pole) mass  $m_0$  of the meson. On the other hand, at high enough temperatures, when the mesonic excitations are completely melted, the spatial meson correlation functions describe the propagation of a free quark-antiquark pair. The screening masses are then given by

$$M_{\text{free}} = \sqrt{m_{q1}^2 + (\pi T)^2} + \sqrt{m_{\bar{q}2}^2 + (\pi T)^2}, \quad (5)$$

where  $m_{q1}$  and  $m_{\bar{q}2}$  are the masses of the quark and anti-quark that form the meson. This form of the screening mass in the non-interacting limit is a direct consequence of the anti-periodic boundary conditions in Euclidean time that are needed for the representation of fermions at non-zero temperature. This leads to the appearance of a smallest non-zero Matsubara frequency,  $\pi T$ , in the quark and anti-quark propagators. As the bosonic meson state is dissolved in the non-interacting limit the screening mass results as the contribution of two independently propagating fermionic degrees of freedom. Thus the transition between these two limiting values of the screening mass can be used as an indicator for the thermal modification and eventual dissolution of mesonic excitations.

In this contribution we study spatial strange-strange, charm-strange and charm-charm meson correlators and screening masses using the Highly Improved Staggered Quark (HISQ) action [24]

with a strange quark mass tuned to its physical value and almost physical, degenerate up and down quark masses. The HISQ action is known to have discretization effects that are smaller than those observed with all other staggered-type actions currently used in studies of lattice QCD thermodynamics [25]. Moreover, the HISQ action is well suited to study heavy quarks on the lattice [24] and turned out to be successful in quantitative studies of charmonium [26] and  $D$  meson properties [27].

## 2. Lattice setup

We calculate meson correlation functions on gauge configurations generated in  $(2+1)$ -flavor QCD using the HISQ action [25]. The strange quark mass  $m_s$  is adjusted to its physical value and the light quark masses are fixed at  $m_l = m_s/20$ , corresponding to  $m_\pi \simeq 160$  MeV and  $m_K \simeq 504$  MeV at zero temperature in the continuum limit [25]. Charm quarks are introduced as valance quarks and we used the HISQ action with the so-called  $\epsilon$ -term for the charm quark [24] which makes our calculations in the heavy quark sector free of tree-level  $\mathcal{O}((am_c)^2)$  discretization errors. Our calculations have been performed on lattices of size  $N_\sigma^3 \cdot N_\tau = 48^3 \cdot 12$ . We consider lattice couplings in the range  $\beta = 6.664$ – $7.280$  which corresponds to temperatures  $T = 138$ – $245$  MeV. Discretization effects on these lattices and for the range of gauge couplings used by us are found to be quite small. To study the spatial correlators at higher temperatures we adopt the fixed-scale approach and perform calculations at  $\beta = 7.280$  for  $N_\tau = 10, 8, 6, 4$  which corresponds to the temperature range  $T = 297$ – $743$  MeV. In all our calculations the spatial extent of lattice was four times the temporal extent:  $N_\sigma = 4N_\tau$ . The lattice spacing and the resulting temperature values,  $T = 1/N_\tau a$ , have been determined using results for the kaon decay constant [25].

In the staggered formulation quarks come in four valance tastes and meson operators are defined as  $J_H = \bar{q}(\Gamma^D \times \Gamma^F)q$ ,  $\Gamma^D$  and  $\Gamma^F$  being products of Dirac Gamma matrices which generate spin and taste structures, respectively [28]. In this study we focus only on local meson operators with  $\Gamma^D = \Gamma^F = \Gamma$ . By using staggered quark fields  $\chi(\mathbf{x})$  at  $\mathbf{x} = (x, y, z, \tau)$  the local meson operators can be written in a simple form  $J_H(\mathbf{x}) = \tilde{\phi}(\mathbf{x})\bar{\chi}(\mathbf{x})\chi(\mathbf{x})$ , where  $\tilde{\phi}(\mathbf{x})$  is a phase factor depending on the choice of  $\Gamma$ . We calculate only the quark-line connected part of the meson correlators since the contribution of the disconnected part either vanishes or is expected to be small in most cases considered in this study (see discussions below). Since staggered meson correlator couples to two different meson excitations with opposite parity, the large distance behavior of the lattice correlator can be described by

$$G(\tau) = A_{\text{NO}}^2 \left( e^{-M-\tau} + e^{-M-(N_\tau-\tau)} \right) - (-1)^\tau A_{\text{O}}^2 \left( e^{-M+\tau} + e^{-M+(N_\tau-\tau)} \right), \quad (6)$$

where the first (second) term on the right-hand-side characterizes a non-oscillating (oscillating) contribution governed by a negative (positive) parity state. Taking the square of the amplitudes ensures their positivity [29]. In Table 1 we summarize the different choices of the phase factor  $\tilde{\phi}$  and the meson states they correspond to. We have considered four channels which we denote as scalar (S), pseudo-scalar (PS), axial vector (AV) and vector (V). The negative parity states in these channels correspond to different tastes of the same physical meson and will thus have nearly degenerate masses if lattice spacing is sufficiently small. For instance, in the  $c\bar{c}$  sector the negative parity states in S and PS channels both correspond to the same  $\eta_c$  state. We will comment on this in more detail later.

In Eq. (6) as well as in Table 1 we assumed that the direction of propagation is the imaginary time  $\tau$ . When discussing spatial correlation functions we assume that the direction of propagation is  $z$ . In this case  $\tau$  in Table 1 and in Eq. (6) should be replaced by  $z$ . Furthermore,  $N_\tau$  should then also be replaced by  $N_\sigma$  in Eq. (6). We calculate meson propagators using point sources as well as corner-wall sources, where on a given times slice the source is set to one

at the origin of each  $2^3$  cube and zero elsewhere. The use of corner-wall sources reduces the contribution of higher excited states and thus allows for a more accurate determination of the screening masses, especially for the positive parity states.

As stated above, in this study we do not include the contribution from the disconnected diagrams. In the case of charmonium the contribution of disconnected diagrams is expected to be small, see e.g. Ref. [30]. For  $s\bar{s}$  mesons disconnected diagrams will cause mixing with the light quark sector in the isospin zero channel. For vector mesons this mixing is known to be very small and the  $\phi$  meson is almost a pure  $s\bar{s}$  state. Thus, neglecting the disconnected diagrams seems to be justified also in this case. Mixing is however large for iso-singlet pseudo-scalar mesons and it is certainly important to include the contribution from the disconnected diagrams when comparing the lattice calculations with the experiment. Alternatively, one can estimate the mass of the un-mixed pseudo-scalar  $s\bar{s}$  meson using leading order chiral perturbation theory  $m_{\eta_{s\bar{s}}}^2 = 2m_K^2 - m_\pi^2 = (686\text{MeV})^2$ , and use this for comparison with the experiment in the PS channel. Not much is known about the mixing between the light and strange sectors for iso-scalar mesons in scalar and axial-vector channels. It is expected that there is strong mixing in the scalar meson sector as well. The mass of the lowest lying  $s\bar{s}$  scalar meson considered in our calculation is about 1.12 GeV as shown in Fig. 2 (explained below). It thus is considerably heavier than the lightest iso-scalar scalar meson  $f_0(980)$  but lighter than the next-to-lightest iso-scalar scalar state  $f_0(1370)$ . However, for the axial-vector meson mass we find good agreement between our calculations and the mass of the  $f_1(1420)$  meson, suggesting that the mixing between the light and strange quark sector is likely to be small in this case. At sufficiently high temperatures we expect that the contribution of disconnected diagrams will become small because of screening effects of the deconfined phase.

The strange quark mass as function of the gauge coupling  $\beta$  was determined in Ref. [25]. We also need to determine the charm quark mass  $m_c$ . For the determination of the charm quark mass we calculate the masses of  $J/\psi$  and  $\eta_c$  mesons for gauge couplings  $\beta = 10/g^2$  in the interval [6.39, 7.28]. We calculate correlation functions at several trial values of the bare charm quark mass in the range  $10 \leq m_c/m_s \leq 14$  using point sources. We then perform linear interpolations in the charm quark mass of the spin-averaged charmonium mass,  $\frac{1}{4}(m_{\eta_c} + 3m_{J/\psi})$  and match them to the physical value. This determines the bare charm quark mass  $am_c$  and the quark mass ratio  $m_c/m_s$  for each value of  $\beta$ . Finally we fit the  $\beta$  dependence of  $am_c$  to a renormalization

**Table 1.** List of meson operators and corresponding physical states in the strange ( $s\bar{s}$ ), strange-charm ( $s\bar{c}$ ) and charm ( $c\bar{c}$ ) sectors. The lightest  $s\bar{s}$  pseudo-scalar state is defined as  $M_{\eta_{s\bar{s}}} = \sqrt{2M_K^2 - M_\pi^2} \sim 686$  MeV which is used to determine the strange quark mass on the lattice.

	$-\tilde{\phi}(x)$	$\Gamma$	$J^{PC}$	$s\bar{s}$	$s\bar{c}$	$c\bar{c}$
$M_-^S$	1	$\gamma_4\gamma_5$	$0^{-+}$			
$M_+^S$		1	$0^{++}$		$D_{s0}^*$	$\chi_{c0}$
$M_-^{\text{PS}}$	$(-1)^{x+y+z}$	$\gamma_5$	$0^{-+}$	$\eta_{s\bar{s}}$	$D_s$	$\eta_c$
$M_+^{\text{PS}}$		$\gamma_4$	$0^{+-}$	–		–
$M_-^{\text{AV}}$	$(-1)^x, (-1)^y$	$\gamma_i\gamma_4$	$1^{--}$			
$M_+^{\text{AV}}$		$\gamma_i\gamma_5$	$1^{+-}$		$D_{s1}$	$\chi_{c1}$
$M_-^V$	$(-1)^{x+z}, (-1)^{y+z}$	$\gamma_i$	$1^{--}$	$\phi$	$D_s^*$	$J/\psi$
$M_+^V$		$\gamma_j\gamma_k$	$1^{+-}$			$h_c$

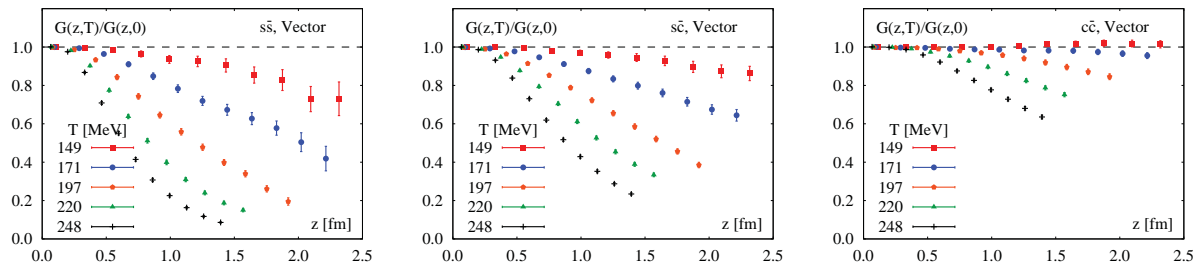


**Figure 1.** The ratio of the non-oscillating (negative parity) part of vector correlator in  $s\bar{s}$  (left),  $s\bar{c}$  (middle) and  $c\bar{c}$  (right) sectors at different temperatures to the corresponding zero temperature results.

group inspired ansatz,

$$am_c^{\text{LCP}} = \frac{c_0 f(\beta) + c_2 (10/\beta) f^3(\beta)}{1 + d_2 (10/\beta) f^2(\beta)}, \quad f(\beta) = \left( \frac{10b_0}{\beta} \right)^{-b_1/(2b_0^2)} \exp\left(-\frac{\beta}{20b_0}\right), \quad (7)$$

where  $b_0$  and  $b_1$  are the coefficients of the QCD beta function. The above formula defines the line of constant physics for the charm quark mass. From our fit we find  $c_0 = 61.0(1.7)$ ,  $c_2 = 2.76(26) \times 10^5$ , and  $d_2 = 3.3(3.7) \times 10^2$ .

We performed calculations of meson correlation functions containing a charm quark in four different channels corresponding to local meson operators (see above) for  $\beta = 6.74, 6.88, 7.03, 7.15$ , and  $7.28$  using point and corner-wall sources. We extracted the zero temperature masses using the ansatz given in Eq. (6) and compared the corresponding results with the experiment. We find that within estimated errors the meson masses agree with the experiment. We also find that the difference between meson masses belonging to different taste multiplets is negligibly small.

### 3. Temperature dependence of spatial meson correlators

Having determined the charm quark masses we can perform calculations of the finite temperature  $s\bar{s}$ ,  $s\bar{c}$  and  $c\bar{c}$  correlation functions in the four different quantum number channels that we have analyzed also at zero temperature.

We start the discussion of our results at non-zero temperature with the temperature dependence of meson correlators. As it was pointed out in Ref. [23], contrary to the temporal correlation functions, spatial correlation functions show visible changes already in the vicinity of the transition temperature even in the case of charmonium. Since staggered meson correlators in each channel contain both negative parity (non-oscillating) and positive parity (oscillating) states, it is important to separate these contributions before studying the temperature dependence of the correlators. One can then form ratios of these contributions at different temperatures and the corresponding zero temperature result. If there is no change in the meson spectral functions, these ratios will be equal to one. As a corollary, deviations of these ratios from unity indicate some medium modification of the meson spectral functions at non-zero temperature.

In Fig. 1, we show the ratio of the negative parity part of the vector correlator in  $s\bar{s}$ ,  $s\bar{c}$  and  $c\bar{c}$  channels and the corresponding zero temperature result. At zero temperature, these non-oscillating parts of vector correlators are dominated by  $\phi$ ,  $D_s^*$  and  $J/\psi$  states, respectively. In the  $s\bar{s}$  sector, We observe a strong decrease of this ratio starting at  $T = 149$  MeV that becomes larger in magnitude with increasing temperature. A somewhat smaller but still significant decrease of

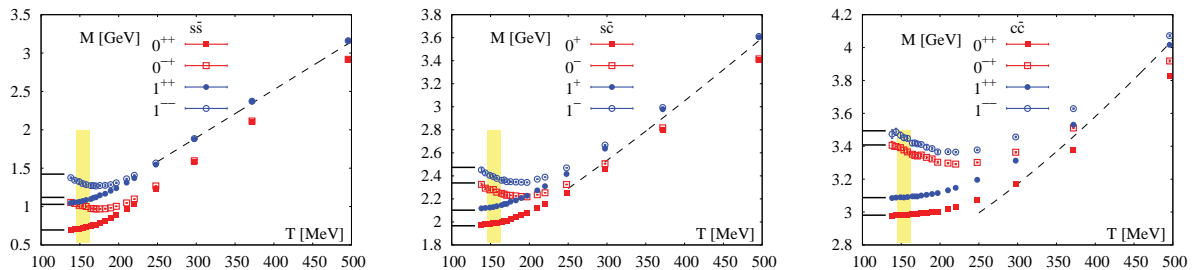


**Figure 2.** Screening masses for different channels in  $s\bar{s}$  (left),  $s\bar{c}$  (middle) and  $c\bar{c}$  (right) sectors as function of the temperature. The solid horizontal lines on the left correspond to the zero temperature meson masses. The dashed line is the free field theory result (see text).

this ratio is also seen in the  $s\bar{c}$  sector. For ratios of charmonium correlators no changes are visible at the lowest temperature (149 MeV), and even at  $T = 171$  MeV the deviations of this ratio from unity are quite small. They become significant only at  $T = 197$  MeV. The results shown in Fig. 1 therefore suggest that there is a sequential pattern of the medium modifications of the meson spectral functions which follows the heavy quark content and the corresponding mass of meson states. For  $s\bar{c}$  and  $c\bar{c}$  mesons we also studied ratios of finite and zero temperature correlators in the pseudo-scalar channel and found results that are very similar to those discussed above for vector mesons. Furthermore, we study the positive parity contributions to the correlators in the scalar channel and the axial-vector channels for  $c\bar{c}$  mesons. At sufficiently low temperatures these ratios encode the in-medium properties of  $\chi_{c0}$  and  $\chi_{c1}$  states. For spatial separations  $z > 0.75$  fm these ratios show a temperature dependence that is similar to that of the corresponding ratio in the vector channel which we have discussed above. The temperature dependence of the ratios at shorter distances,  $z < 0.75$  fm is significantly stronger than that in the vector and pseudo-scalar channels, providing some hints for the expected sequential suppression pattern of different charmonium states. Clearly a more detailed analysis of the spatial correlators is needed to clarify this issue, which will be discussed in the next section.

#### 4. Large distance behavior of spatial meson correlators and screening masses

We fit the large distance behavior of the spatial correlators using Eq. (6) and extract screening masses in various channels for  $s\bar{s}$ ,  $s\bar{c}$  and  $c\bar{c}$  mesons. In our study of PS and V screening masses, we use point and corner-wall sources. For  $c\bar{c}$  sector the difference between the point and corner-wall sources is quite small. It typically is around 0.4%, except for the three highest temperature, where it reaches 3%. Similarly in the  $s\bar{c}$  sector, the difference between point and wall sources is typically about 1% for all temperatures except the three highest ones, where it is 3%. Larger differences between point and wall sources are seen in the  $s\bar{s}$  sector, where they reach 3% at the highest five temperatures, and are about 1% at other temperatures. Therefore, we will use the results from corner-wall sources when presenting our results on the screening masses in the PS and V channels. In the S and AV channels screening masses can be reliably extracted only when using the corner-wall sources. The effects of taste symmetry breaking are only visible for the negative parity states in PS and S channels at low temperatures, where they are about 1.5%. For temperature above 200 MeV we do not find any statistically significant effect of taste splitting.

All our results on screening masses in the  $s\bar{s}$ ,  $s\bar{c}$  and  $c\bar{c}$  are shown in Fig. 2. The error bars in the figure indicate the statistical and systematic errors added in quadrature. We expect that at very high temperature the screening masses are given by Eq. (5). We show the free theory (leading order perturbative) result as dashed lines in Fig. 2. For this we need to specify the quark

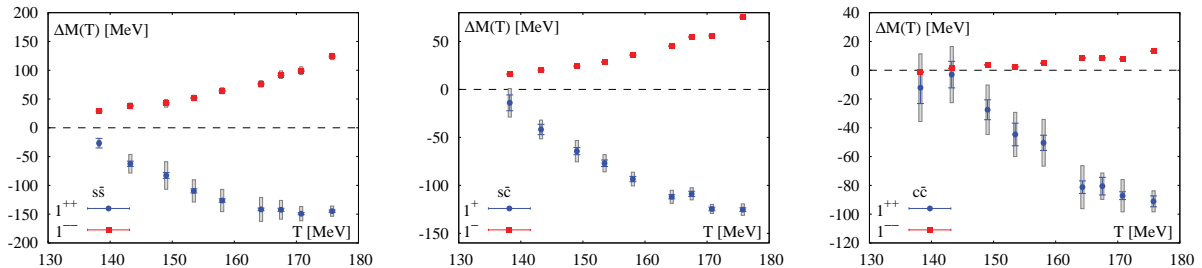


**Figure 3.** The difference  $\Delta M(T) = M(T) - m_0$  for vector and axial-vector channels in  $s\bar{s}$  (left),  $s\bar{c}$  (middle) and  $c\bar{c}$  (right) sectors as function of the temperature.

masses. The quark masses depend on the renormalization scale which is not fixed at leading order. A natural choice of the renormalization scale would be to identify it with the lowest scale in the problem provided that this lowest scale is still in the perturbative region. In our case there are two relevant energy scales, the charm quark mass  $m_c$ , and the thermal scale which here is taken to be  $2\pi T$ . For temperatures  $T > 200$  MeV both scales are comparable. Therefore, we could take the charm quark mass as the renormalization scale and the corresponding value  $m_c(\bar{\mu} = m_c) = 1.275$  GeV from PDG [31]. Using the ratio of charm to strange quark mass  $m_c/m_s = 11.85$  [32] and the above value, we can determine the value of the strange quark mass at the same renormalization scale to be  $m_s = 0.108$  GeV. This completely specifies our free theory prediction.

As one can see from Fig. 2, there are three distinct regions: the low temperature region, where the screening masses are close to the corresponding vacuum masses (solid lines), the intermediate temperature region, where we see significant changes in the value of the screening masses with respect to the corresponding vacuum masses, and finally, the high temperature region, where the screening masses are close to the free theory result (dashed lines). In the high temperature region, there clearly are no meson bound states anymore. The onset of the high temperature behavior is different in different sectors. In the  $s\bar{s}$  sector it starts at around  $T = 210$  MeV. In the  $s\bar{c}$  sector it starts at  $T = 250$  MeV, while in  $c\bar{c}$  sector it starts at  $T > 300$  MeV. As the temperature increases, we see that the screening masses corresponding to negative parity states increase monotonically, while the screening masses in the positive parity states first decrease before starting to rise towards the asymptotic high temperature values. In the intermediate temperature region the screening masses of opposite parity partners start to approach each other and we observe a significant rearrangement of the ordering of screening masses in different channels. At sufficiently high temperatures the PS and S as well as V and AV screening masses become degenerate. In the  $s\bar{s}$  sector this is evident for  $T > 220$  MeV, while for the two other sectors it happens at higher temperatures because in these cases the effect of the explicit breaking of parity by the quark masses is much larger. In the high temperature region the screening masses in the PS channel are smaller than the screening masses in the V channel. This behavior has been observed previously in lattice calculations [22] and in calculations using Dyson-Schwinger equations [33]. It persists to temperatures as high as 800 MeV, see e.g. Ref. [22].

To see in detail the modification of screening masses in the low and intermediate temperature regions it is convenient to consider the difference between the screening mass and the corresponding vacuum masses  $m_0$  calculated at  $T = 0$

$$\Delta M(T) = M(T) - m_0. \quad (8)$$

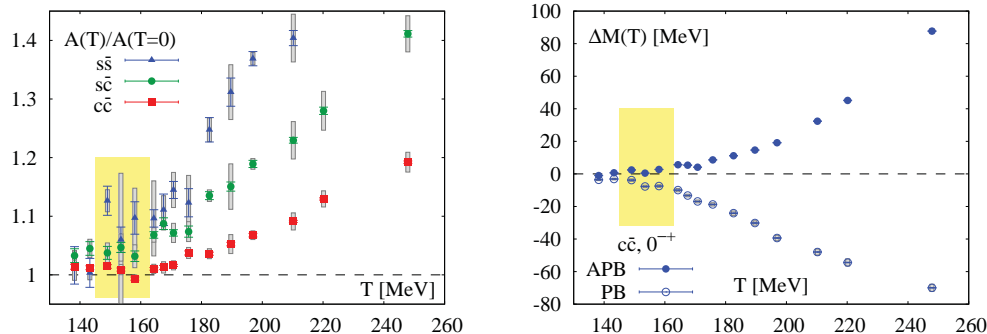


**Figure 4.** The right panel shows the ratio of the amplitudes of vector spatial meson correlators calculated at finite temperature and zero temperature. The left panel shows the difference between the pseudo-scalar screening mass and the corresponding zero temperature mass  $\Delta M(T) = M(T) - m_0$  for anti-periodic (filled symbols) and periodic (open symbols) boundary conditions

It is tempting to interpret this difference as the change in the binding energy of meson states, however, the relation between the screening mass and the pole mass only holds as long as there is a well defined bound state. Nonetheless,  $\Delta M$  could provide some constraints on the change of the binding energy in the low and intermediate temperature regions. We show our results for  $\Delta M(T)$  for vector and axial-vector  $s\bar{s}$ ,  $s\bar{c}$  and  $c\bar{c}$  mesons in Fig. 3. The error bars and gray bands indicate the statistical and systematic errors, respectively. In all cases  $\Delta M$  increases for negative parity states and decreases for positive parity states. The absolute value of  $\Delta M$  is the largest for  $s\bar{s}$  meson and is the smallest for  $c\bar{c}$  mesons, i.e. it follows the expected sequential pattern with respect of the heavy quark content. Note, that the absolute size of  $\Delta M$  is about the same for negative and positive parity states in the  $s\bar{s}$  sector. In the charm-strange sector  $|\Delta M|$  is slightly larger for positive parity state. For charmonium the picture is different,  $\Delta M$  remains quite small for  $T < 200$  MeV in the vector channel, while we see large decrease in  $\Delta M$  for the axial-vector channel starting around  $T = 160$  MeV. We also inspected the behavior of  $\Delta M$  in the scalar and pseudo-scalar channels and found a behavior that is almost identical to that in the axial-vector and vector channels. Thus, in the charmonium case the temperature dependence of  $\Delta M$  provides some hints for sequential suppression: it shows large decrease at  $T > 160$  MeV for scalar and axial vector channels corresponding to 1P charmonium states ( $\chi_{c0}$  and  $\chi_{c1}$ ) and very little change in the pseudo-scalar and vector channels corresponding to 1S charmonium states ( $\eta_c$  and  $J/\psi$ ).

The amplitudes  $A_{NO}$  and  $A_O$  appearing in Eq. (6) are related to the wave function of meson states in the zero temperature limit. In the case of point sources and mesons consisting of heavy quarks they are proportional to the wave function at the origin and the derivative of the wave function at origin. Therefore, if we are interested in melting of meson states at high temperature it is worth to study the temperature dependence of this amplitudes. In Fig. 4 we show the ratios of the amplitude  $A_{NO}$  for the spatial meson correlators in the vector channel to the corresponding zero temperature result. If meson states exist in the medium with little or no modifications this ratio should be close to one. For the strange and strange-charm mesons we see that there are deviations of this ratio from one already at relatively low temperatures and these deviations are increasing with increasing temperature. For charmonium the ratio of the amplitude to the zero temperature amplitude is very close to one up to temperature of about 170 MeV, and slowly increases above that temperature. Only at temperatures above 200 MeV the deviations of this ratio from unity are similar to the ones observed in strange and strange-charm

sectors in the transition region. This suggests that melting of the  $J/\psi$  happens for  $T > 200$  MeV.

Finally, let us discuss the dependence of charmonium screening masses on the temporal boundary conditions. So far we used anti-periodic boundary conditions for valence charm quarks, i.e. we considered them to be in thermal equilibrium. In heavy ion experiments charm quarks are most likely not in thermal equilibrium due to their large mass and large relaxation times. The existence of charmonium bound state in the medium with a certain temperature does not depend on whether the charm quarks are thermalized or not. If the temperature is not too high one can use NRQCD to study heavy quark bound state. In this approach no boundary conditions are imposed on the heavy quark [34] but the sequential suppression pattern has been observed. Thus, if charmonium state exists in the medium the spatial correlation function and screening masses should be insensitive to the temporal boundary conditions. It was pointed out in Ref. [23] if bound states are melted meson screening masses will be very sensitive to the temporal boundary conditions. Asymptotically the quadratic difference of the screening masses calculated with anti-periodic and periodic boundary conditions will approach  $(2\pi T)^2$  [23]. In Fig. 4 we show the charmonium screening masses in the pseudo-scalar channel calculated using anti-periodic and periodic boundary conditions. There is very little sensitivity to the boundary conditions for  $T < 170$  MeV. Above that temperature we see clear sensitivity of the pseudo-scalar screening mass to the boundary conditions, which becomes quite large for  $T > 200$  MeV possibly indicating dissolution of the  $\eta_c$  state at these temperatures. The results in the vector channel are very similar. We also see sensitivity to the boundary conditions in the scalar and axial-vector charmonium screening masses. But due to large errors in the corresponding screening masses it is more difficult to quantify this sensitivity.

## 5. Conclusions

We studied spatial meson correlation functions at non-zero temperature for  $s\bar{s}$ ,  $s\bar{c}$  and  $c\bar{c}$  mesons with the aim to find out at what temperatures these mesons dissolve. We studied the spatial correlation functions in different ways: comparing them directly to the zero temperature results, studying their large distance behavior and extracting the corresponding screening masses and amplitudes, as well as studying the sensitivity to the temporal boundary conditions. We see that the size of medium effects in the spatial correlators and screening masses in different sectors follows a sequential pattern that corresponds to the heavy quark content. We find, however, that both  $s\bar{s}$  and charm strange mesons are effected by the medium already at relatively low temperatures and dissolve at temperature close to the transition temperature. Contrary, the 1S charmonium states ( $J/\psi$  and  $\eta_c$ ) do not seem to be affected by the medium up to temperatures of about 170 MeV and most likely dissolve at temperatures somewhat higher than 200 MeV. The correlators and the screening masses corresponding to 1P charmonium ( $\chi_c$ ) states show larger temperature dependence than the ones corresponding to 1S states. In particular, the screening masses corresponding to 1P charmonium states show large temperature dependence just above the transition temperature. Thus, we see some hints of the expected charmonium suppression from our study of spatial correlation functions.

## Acknowledgments

Numerical calculations were carried out on the USQCD Clusters at the Jefferson Laboratory, USA, the NYBlue at the Brookhaven National Laboratory, USA and in NERSC at Lawrence Berkeley National Laboratory, USA. This work was supported by through the Contract No. DE-AC02-98CH10886 with the U.S. Department of Energy and the Bundesministerium für Bildung und Forschung under grant 05P12PBCTA, and the EU Integrated Infrastructure Initiative Hadron-Physics3. Partial support for this work was also provided through Scientific Discovery through Advanced Computing (SciDAC) program funded by U.S. Department of Energy, Office

of Science, Advanced Scientific Computing Research (and Basic Energy Sciences/Biological and Environmental Research/High Energy Physics/Fusion Energy Sciences/Nuclear Physics).

- [1] Petreczky P 2012 *J.Phys.* **G39** 093002 (*Preprint* 1203.5320)
- [2] Philippsen O 2013 *Prog.Part.Nucl.Phys.* **70** 55–107 (*Preprint* 1207.5999)
- [3] Detar C E and Kogut J B 1987 *Phys.Rev.Lett.* **59** 399
- [4] Detar C E and Kogut J B 1987 *Phys.Rev.* **D36** 2828
- [5] Laine M and Vepsalainen M 2004 *JHEP* **0402** 004 (*Preprint* hep-ph/0311268)
- [6] Brandt B, Francis A, Laine M and Meyer H 2014 *JHEP* **1405** 117 (*Preprint* 1404.2404)
- [7] Matsui T and Satz H 1986 *Phys.Lett.* **B178** 416
- [8] Sharma R, Vitev I and Zhang B W 2009 *Phys.Rev.* **C80** 054902 (*Preprint* 0904.0032)
- [9] Asakawa M, Hatsuda T and Nakahara Y 2001 *Prog. Part. Nucl. Phys.* **46** 459–508 (*Preprint* hep-lat/0011040)
- [10] Wetzorke I, Karsch F, Laermann E, Petreczky P and Stickan S 2002 *Nucl.Phys.Proc.Suppl.* **106** 510–512 (*Preprint* hep-lat/0110132)
- [11] Asakawa M, Hatsuda T and Nakahara Y 2003 *Nucl. Phys.* **A715** 863–866 (*Preprint* hep-lat/0208059)
- [12] Asakawa M and Hatsuda T 2004 *Phys. Rev. Lett.* **92** 012001 (*Preprint* hep-lat/0308034)
- [13] Datta S, Karsch F, Petreczky P and Wetzorke I 2004 *Phys. Rev.* **D69** 094507 (*Preprint* hep-lat/0312037)
- [14] Jakovac A, Petreczky P, Petrov K and Velytsky A 2007 *Phys. Rev.* **D75** 014506 (*Preprint* hep-lat/0611017)
- [15] Aarts G, Allton C, Oktay M B, Peardon M and Skullerud J I 2007 *Phys. Rev.* **D76** 094513 (*Preprint* 0705.2198)
- [16] Ding H, Francis A, Kaczmarek O, Karsch F, Satz H *et al.* 2012 *Phys.Rev.* **D86** 014509 (*Preprint* 1204.4945)
- [17] Petreczky P, Miao C and Mocsy A 2011 *Nucl.Phys.* **A855** 125–132 (*Preprint* 1012.4433)
- [18] de Forcrand P *et al.* (QCD-TARO Collaboration) 2001 *Phys.Rev.* **D63** 054501 (*Preprint* hep-lat/0008005)
- [19] Boyd G, Gupta S, Karsch F and Laermann E 1994 *Z.Phys.* **C64** 331–338 (*Preprint* hep-lat/9405006)
- [20] Pushkina I *et al.* (QCD-TARO Collaboration) 2005 *Phys.Lett.* **B609** 265–270 (*Preprint* hep-lat/0410017)
- [21] Iida H, Maezawa Y and Yazaki K 2010 *PoS LATTICE2010* 189 (*Preprint* 1012.2044)
- [22] Cheng M, Datta S, Francis A, van der Heide J, Jung C *et al.* 2011 *Eur.Phys.J.* **C71** 1564 (*Preprint* 1010.1216)
- [23] Karsch F, Laermann E, Mukherjee S and Petreczky P 2012 *Phys.Rev.* **D85** 114501 (*Preprint* 1203.3770)
- [24] Follana E *et al.* (HPQCD Collaboration, UKQCD Collaboration) 2007 *Phys.Rev.* **D75** 054502 (*Preprint* hep-lat/0610092)
- [25] Bazavov A, Bhattacharya T, Cheng M, DeTar C, Ding H *et al.* 2012 *Phys.Rev.* **D85** 054503 (*Preprint* 1111.1710)
- [26] Davies C, Donald G, Dowdall R, Koponen J, Follana E *et al.* 2012 *PoS ConfinementX* 288 (*Preprint* 1301.7203)
- [27] Bazavov A *et al.* (Fermilab Lattice and MILC Collaborations) 2013 (*Preprint* 1312.0149)
- [28] Altmeyer R *et al.* (MT(c) collaboration) 1993 *Nucl.Phys.* **B389** 445–512
- [29] Lepage G, Clark B, Davies C, Hornbostel K, Mackenzie P *et al.* 2002 *Nucl.Phys.Proc.Suppl.* **106** 12–20 (*Preprint* hep-lat/0110175)
- [30] Levkova L and DeTar C 2011 *Phys.Rev.* **D83** 074504 (*Preprint* 1012.1837)
- [31] Beringer J *et al.* (Particle Data Group) 2012 *Phys.Rev.* **D86** 010001
- [32] Davies C, McNeile C, Wong K, Follana E, Horgan R *et al.* 2010 *Phys.Rev.Lett.* **104** 132003 (*Preprint* 0910.3102)
- [33] Wang K I, Liu Y x, Chang L, Roberts C D and Schmidt S M 2013 *Phys.Rev.* **D87** 074038 (*Preprint* 1301.6762)
- [34] Aarts G, Kim S, Lombardo M, Oktay M, Ryan S *et al.* 2011 *Phys.Rev.Lett.* **106** 061602 (*Preprint* 1010.3725)